

# DYNAMIC APERTURE STUDIES FOR VERTICAL FIXED FIELD ACCELERATORS

M. Vanwelde\*, C. Hernalsteens<sup>1</sup>, E. Gnacadja, E. Ramoisiaux, R. Tesse, N. Pauly  
 Service de Métrologie Nucléaire, Université libre de Bruxelles, Brussels, Belgium  
<sup>1</sup>CERN, European Organization for Nuclear Research, Geneva, Switzerland

## Abstract

Vertical orbit excursion Fixed Field Accelerators (vFFAs) feature highly nonlinear magnetic fields and strong transverse motion coupling. The detailed study of their Dynamic Aperture (DA) requires computation codes allowing long-term tracking and advanced analysis tools to take the transverse motion linear and nonlinear coupling into account. This coupling completely transforms the beam dynamics compared to a linear uncoupled motion, and an explicit definition of the DA is needed to characterize the performance and limitations of these lattices. A complete study of the DA in the 4D phase space in highly nonlinear and strongly coupled machines must give a measure of the stability domain but also means to assess the operating performance in the physical coupled space. This work presents a complete set of methods to perform such detailed analysis. These methods were explored and compared to compute and characterize the DA of an example vFFA lattice. The whole procedure can be further applied to evaluate DA using realistic models of the magnetic fields, including fringe fields and errors.

## INTRODUCTION

vFFAs [1, 2] feature magnetic fields increasing exponentially in the vertical direction, such that the orbits are stacked along the vertical plane. Their magnetic field satisfies the scaling condition  $B = B_0 \exp[k(z - z_0)]$ , where  $k = (1/B)(\partial B/\partial z)$  is the normalized field gradient,  $z_0$  is a vertical reference position and  $B_0$  is the bending field at that reference position. vFFA magnetic fields exhibit longitudinal and skew quadrupolar components, inducing strongly coupled linear optics that requires adequate coupling parametrization [3] for studying their linear beam dynamics [4]. In addition, the exponential form produces a highly nonlinear field, resulting in nonlinear coupling between the linearly decoupled planes. The detailed study of their nonlinear beam dynamics, including the characterization of their DA, must account for this linear and nonlinear coupling. The DA is practically defined as the phase space region where the motion of the particles remains bounded over a finite number of turns. As vFFAs manifest linear and nonlinear coupling, the particle transverse motion explores the full 4D phase space, and the stability domain is a 4D volume without a well-defined boundary [5, 6]. In Refs. [6, 7], different methods are explored to compute this 4D volume, from precise CPU-intensive methods consisting in scanning all phase space variables to fast methods that make use of the time dynamics to avoid scanning over the phase plane angles. To evaluate the stability domain phase space complexity, the 4D volume should be accompanied by metrics representing the topology of this phase space. As the stability domain

can be significantly deformed, another DA definition, which takes the minimal amplitude ensuring all particles in the corresponding hypersphere survive 1000 turns, can be explored and has a better interpretation in terms of beam injection in the coupled physical space.

This work proposes a complete procedure to study the DA in highly nonlinear and strongly coupled machines. This procedure is illustrated on the vFFA lattice presented in Ref.[2], which is the first design of the vFFA proton driver prototype (FETS-FFA) studied under the ISIS-II project [8–10]. The 4D stability domain volume estimates using different methods are computed and compared. Then, a method to compute a more practical interpretable DA is explored. Finally, several metrics to characterize the phase space stability domain in terms of its diffuse character and spectral behavior are established and studied in detail. All the results are obtained using Zgoubi [11–13] combined with its python interface Zgoubidoo [14]. This procedure paves the way for future in-depth studies of vFFA machines.

## ESTIMATE OF THE 4D STABILITY DOMAIN

In this work, we fully characterize the DA on 1000 turns<sup>1</sup> around the 10-cell vFFA prototype lattice presented in Ref. [2]. We used the VFFA Zgoubi keyword with an integration step of 0.5 cm for accurate tracking, and a nominal energy of 3 MeV; the lattice closed orbit and linear beam dynamics were already explored with Zgoubi in Ref. [4]. Because of the nonlinear coupling, the particles oscillate in both linearly decoupled planes so that the particle initial coordinates with respect to the closed orbit read:

$$u = r \cos(\alpha) \cos(\theta_1), \quad p_u = r \cos(\alpha) \sin(\theta_1), \quad (1)$$

$$v = r \sin(\alpha) \cos(\theta_2), \quad p_v = r \sin(\alpha) \sin(\theta_2), \quad (2)$$

where  $r$  is the amplitude in the 4D space,  $\theta_1, \theta_2$  are the angles in each decoupled plane, and  $\alpha$  characterizes the ratio of the amplitudes in both linearly decoupled planes [6]. The DA is defined by the radius of the 4D hypersphere with the same volume as the phase space stability domain [6].

To compute the volume of the stability domain, we have used the methods detailed in Refs. [6, 7] and referred to as “Direct integration with scan over phase space variables” and “Integration over the dynamics”. Scanning over the full 4D phase space is the more precise and rigorous method, but is highly CPU-intensive as it requires evaluating a large number of orbits to scan a sufficiently high number of directions  $(\alpha, \theta_1, \theta_2)$ . The integration over the dynamics avoids scanning over  $\theta_1$  and  $\theta_2$  and performs an average over the iterates from the tracking of the maximum amplitude particles for several  $\alpha$  with  $\theta_1 = \theta_2 = 0$ . As the variable

\* marion.vanwelde@ulb.be

<sup>1</sup> Reference [2] shows that the 2D-DAs converge for 1000 turns.

Table 1: Parameters and results for the methods to estimate the stability domain. The 4D volumes are normalized by  $(\beta\gamma)^2$ .

	Direct Integration		C) Integration over the dynamics
	A) Scan over phase space variables	B) Random sampling	
Initial conditions	~ 3 million orbits scanned to find the maximum amplitude in $r = [0, 0.06]$ surviving 1000 turns for each point of the integration mesh. It gives 157 339 particles with maximum amplitude.	30 million random initial conditions uniformly distributed in a 4D hypersphere with $r = 0.06$ m, resulting in 558000 initial conditions stable on 1000 turns.	1800 orbits evaluated to find the 90 particles with the maximum amplitude that survives 1000 turns for each $\alpha$ in $[0^\circ, 90^\circ]$ with $\theta_1 = \theta_2 = 0$ .
Integration mesh	$(\Delta\alpha, \Delta\theta_1, \Delta\theta_2) = (5^\circ, 4^\circ, 4^\circ)$ .	$(\Delta\alpha, \Delta\theta_1, \Delta\theta_2) = (7.5^\circ, 10.3^\circ, 10.3^\circ)$ .	$(\Delta\alpha, \Delta\theta_1, \Delta\theta_2) = (11.25^\circ, 27.7^\circ, 27.7^\circ)$ .
DA (volume)	727.15 mm <sup>2</sup> mrad <sup>2</sup> $\pi^2$ .	1087.91 mm <sup>2</sup> mrad <sup>2</sup> $\pi^2$ .	697.05 mm <sup>2</sup> mrad <sup>2</sup> $\pi^2$ .
DA (equivalent radius)	6.175 mm.	6.83 mm.	6.11 mm.
Pros and cons	- Find simply connected stability domain - CPU-intensive - Accurate DA estimate	- Outliers increase the volume - CPU-intensive - Poor DA estimate	- Non-uniform phase distribution - Less computationally demanding - Reliable DA estimate

scan only allows for finding the largest connected stability domain, we also use a third method, namely the random sampling method, to obtain the stability domain that includes the points lying in areas disconnected from the main stability domain. This method tracks many particles with random initial coordinates uniformly distributed in a 4D hypersphere and retains the initial conditions that survive 1000 turns, before integrating on an adequate mesh<sup>2</sup>. These three methods are summarized in Table 1 with their initial conditions, including the particle initial coordinates. The results in terms of the DA 4D volume and equivalent radii are also shown.

The most accurate 4D volume estimate is given by the phase space variable scan but requires evaluating a large number of orbits. The random sampling method is also CPU-intensive and provides a poor volume estimate (relative error of ~50% compared to the scan method) because it includes outliers, as shown in Fig. 1(a). These outliers increase the total volume because the mesh used for integration is coarse, leading to low accuracy. The integration over the dynamics provides a suitable volume estimate (relative error of 4.14% compared to the scan method) while saving considerable CPU time. Nevertheless, it requires to use an adequate mesh (at least one iteration per bin) to account for the non-uniformity of the iteration phases. This method appears to be the best method when the DA is computed to compare several lattices or working points. Nevertheless, once a lattice design and working point must be studied in detail, the phase space variables scan method must be used to have the most accurate estimate of the stability domain.

The stability domain can deviate significantly from a hypersphere due to phase space distortions. To find the effective radius of the acceptance hypersphere of the machine that survives 1000 turns, the DA can be defined as the maximum 4D-hypersphere that fits inside the stability domain. Without imposing that the hypersphere center corresponds to the closed orbit, we found a hypersphere with a radius of 16.6 mm<sup>1/2</sup>mrad<sup>1/2</sup>, corresponding to normalized volume and radius of 242.98 mm<sup>2</sup>mrad<sup>2</sup> $\pi^2$  and 4.695 mm<sup>1/2</sup>mrad<sup>1/2</sup>; it corresponds to ~ 33% of the 4D volume estimate of the stability domain. This difference characterizes the phase space distortion due to the nonlinearity of the vFFA lattice.

<sup>2</sup> The integration mesh contains at least one initial condition in each bin which retains the coordinate with the largest radius.

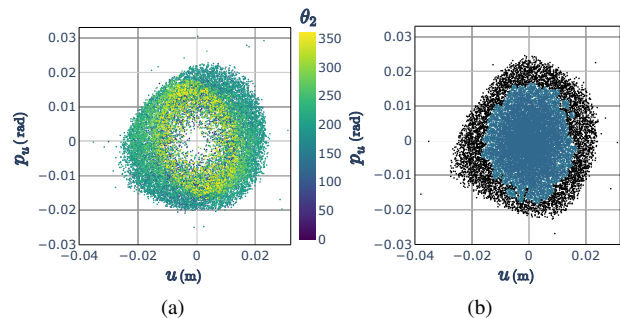


Figure 1: (a) Surviving initial conditions for the random sampling method in  $(u - p_u)$  for  $\alpha = 35^\circ$ . (b) The clustering method was applied to these point 2D coordinates for all  $\alpha$ . The outliers detached from the connected stability zone may correspond to points of the separatrix surrounding higher-order hyperbolic fixed points.

## DA QUALITY FACTORS

We explored several ways to qualify the 4D phase space stability domain and evaluate its complexity. The metrics and analysis tools we have used are summarized in Table 2.

We first applied a frequency analysis method. We computed the frequency spectrum for each stable particle from a turn-by-turn frequency analysis of the particle motions in the  $u$  and  $v$  directions on 1024 cells with pyNAFF [15]. The analysis of the main frequencies suggests the absence of stability islands in the connected stability domain. To quantify the lattice nonlinear nature, we have also computed the ratio between the amplitude of the main peak and the total amplitude in the spectrum for each particle whose main frequencies are close to the design tunes. If most of the power lies in the main FFT peak, the lattice is close to a linear lattice, while for (weakly) chaotic motion, a large part of the particle signal power lies in the FFT secondary peaks. The median ( $f$ ) of the  $u$  and  $v$  ratio distributions are respectively 0.776 and 0.915, as shown in Fig. 2, indicating that the motion in the  $u$ -plane is more affected by non-linearities and exhibits a behavior closer to chaotic behavior.

To gain insight into the global system dynamics, we have also computed the diffusion coefficient for each point. This coefficient characterizes the diffusion of the cell tunes over 1024 cells and is defined as  $D = \log_{10}(\sqrt{\Delta Q_u^2 + \Delta Q_v^2})$ , where  $\Delta Q_u$  and  $\Delta Q_v$  are the difference in the eigentunes computed on the two halves of the turn data [16]. The global

Table 2: Metrics and analysis tools to characterize the complexity of the phase space stability domain. The letters A, B, and C refer to the methods to compute the 4D DA estimate.

	Frequency Analysis		Clustering Metric
	Main frequencies & non linearities	Diffusion coefficient metric	
Goals	- Detection of stability islands - Characterization of the lattice non-linearity	- Characterization of the system global dynamics - Identification of harmful resonances	Characterization of the phase space distribution with its different dynamics zones
Results	- No stability islands $-f_u = 0.776, f_v = 0.915$	- $g = 0.9865$ (A), $0.9857$ (B), $0.9965$ (C) - Resonances: $-4\nu_1 + 2\nu_2 = 1$ , $5\nu_1 + 3\nu_2 = 3$	- No characteristic dynamics zones $-h_u = 0.795, h_v = 0.871$
Observations	Only characterizes the $u$ or the $v$ motion at a time.	- Approximately constant for all distributions - Difficult choice of threshold	- The outliers influence the initial parameters - Depends on the number of stable particles

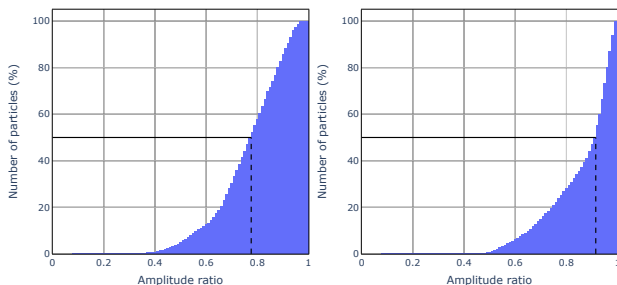


Figure 2: Cumulative histograms of the ratio between the amplitude in the main peak and the total amplitude in the spectrum for each particle whose main frequencies are close to the machine cell tunes. These histograms correspond to the motion in the  $u$ -direction (a) and the  $v$ -direction (b).

diffusion is summarized by comparing the diffusion coefficient of each point to a threshold set to -6, and computing the metric  $g = \frac{\text{Number of "non-diffuse" points}}{\text{Total number of points}}$ . The constancy of this metric across the different 4D estimate methods, shown in Table 2, suggests that it is a reliable quality factor.

We also performed a frequency map analysis (FMA) [17, 18]. The resonances that seem to affect and limit the DA are the difference resonance  $-4\nu_1 + 2\nu_2 = 1$  and the sum resonance  $5\nu_1 + 3\nu_2 = 3$ , as shown in Fig. 3. These high-order resonances could explain the outliers appearing in the random sampling method, which may correspond to points of the separatrix surrounding high-order hyperbolic fixed points. The importance of the high-order resonances in vFFAs is not yet fully understood, and further studies are needed to mitigate them to increase the DA of such lattices.

Finally, we have used the scikit-learn “DBSCAN (Density-Based Spatial Clustering of Applications with Noise)” function [19] to divide the points into clusters of similar density and noise. We have then computed the metric  $h = \frac{\text{Number of points in clusters}}{\text{Total number of points}}$ . It characterizes the spatial diffusive aspect of the point distribution obtained with the random sampling method. We have applied the clustering in the 2D linearly decoupled planes, as illustrated in Fig. 1(b), and obtained clustering metrics of 0.795 and 0.871, which are coherent with the values of the FFT amplitude ratio distribution medians. The clustering is a more qualitative tool because it strongly depends on the initial parameters and on the number of points in the distribution, but it provides better visualization and informs on the different dynamics regions in phase space.

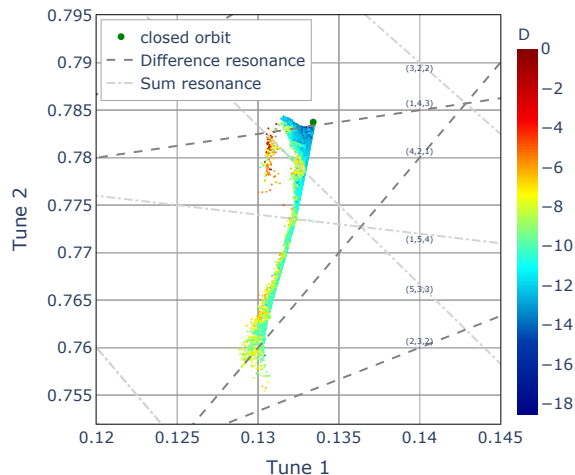


Figure 3: Tune diffusion map for the random sampling method. The DA is affected by the difference resonance  $-4\nu_1 + 2\nu_2 = 1$  and by the sum resonance  $5\nu_1 + 3\nu_2 = 3$ .

## CONCLUSION

A complete procedure to perform a detailed analysis and fully characterize the DA of vFFA lattices has been presented. It includes the computation of a 4D estimate of the stability domain volume, of metrics to evaluate the stability domain quality, and of the volume of the largest 4D-hypersphere inscribed into the stability domain to recover the DA meaning in terms of beam injection in the coupled space. The whole procedure has been successfully used to thoroughly investigate the DA of a vFFA prototype ring. We have obtained a DA volume of  $727.15 \text{ mm}^2 \text{ mrad}^2 \pi^2$ . The volume of the largest inscribed hypersphere is only 33% of the stability domain volume, indicating a large phase space distortion due to the lattice non-linearities. These non-linearities also result in high-order resonances that limit the DA. It can be detected by the FMA and highlighted by the random sampling method. The whole procedure can be extensively used in future studies to characterize the nonlinear beam dynamics of highly nonlinear and coupled machines, from the design stage to the in-depth study of one lattice with realistic models of magnetic fields, including fringe fields and errors.

## ACKNOWLEDGMENTS

Marion Vanwelde is a Research Fellow of the Fonds de la Recherche Scientifique - FNRS.

## REFERENCES

- [1] S. Brooks, “Vertical orbit excursion fixed field alternating gradient accelerators,” *Phys. Rev. ST Accel. Beams*, vol. 16, no. 8, p. 084001, 2013.  
doi:10.1103/PhysRevSTAB.16.084001
- [2] S. Machida, D. J. Kelliher, J.-B. Lagrange, and C. T. Rogers, “Optics design of vertical excursion fixed-field alternating gradient accelerators,” *Physical Review Accelerators and Beams*, vol. 24, no. 2, p. 021601, 2021.  
doi:10.1103/PhysRevAccelBeams.24.021601
- [3] M. Vanwelde, C. Hernalsteens, S. A. Bogacz, S. Machida, and N. Pauly, *Review of coupled betatron motion parametrizations and applications to strongly coupled lattices*, 2022.  
doi:10.48550/ARXIV.2210.11866
- [4] M. Vanwelde, C. Hernalsteens, F. Méot, N. Pauly, and R. Tesse, “Modeling and implementation of vertical excursion FFA in the Zgoubi ray-tracing code,” *Nucl. Instrum. Methods Phys. Res., Sect. A*, vol. 1047, p. 167829, 2023.  
doi:10.1016/j.nima.2022.167829
- [5] A. Bazzani, M. Giovannozzi, and E. H. Maclean, “Analysis of the non-linear beam dynamics at top energy for the CERN Large Hadron Collider by means of a diffusion model,” *The European Physical Journal Plus*, vol. 135, no. 1, p. 77, 2020.  
doi:10.1140/epjp/s13360-020-00123-2
- [6] E. Todesco and M. Giovannozzi, “Dynamic aperture estimates and phase-space distortions in nonlinear betatron motion,” *Physical Review E*, vol. 53, no. 4, pp. 4067–4076, 1996.  
doi:10.1103/PhysRevE.53.4067
- [7] M. Giovannozzi and E. Todesco, “Numerical methods to estimate the dynamic aperture,” *Particle Accelerators*, vol. 54, pp. 203–212, 1996.
- [8] J. Thomason *et al.*, ISIS II “Working Group Report”, <https://www.isis.stfc.ac.uk/Pages/isis-iiworking-group-report16266.pdf>.
- [9] J.-B. Lagrange *et al.*, “Progress on Design Studies for the ISIS II Upgrade,” in *Proc. IPAC’19*, Melbourne, Australia, May 2019, pp. 2075–2078.  
doi:10.18429/JACoW-IPAC2019-TUPTS068
- [10] C. M. Warsop *et al.*, “Studies for Major ISIS Upgrades via Conventional RCS and Accumulator Ring Designs,” in *Proc. IPAC’18*, Vancouver, Canada, Apr.-May 2018, pp. 1148–1150. doi:10.18429/JACoW-IPAC2018-TUPAL058
- [11] F. Méot, “The ray-tracing code Zgoubi,” *Nucl. Instrum. Methods Phys. Res., Sect. A*, vol. 427, no. 1-2, pp. 353–356, 1999.  
doi:10.1016/S0168-9002(98)01508-3
- [12] F. Méot and J. Berg, *Zgoubi*, <http://sourceforge.net/projects/zgoubi/>, 2020.
- [13] F. Méot, “The ray-tracing code Zgoubi – Status,” *Nucl. Instrum. Methods Phys. Res., Sect. A*, vol. 767, pp. 112–125, 2014. doi:10.1016/j.nima.2014.07.022
- [14] C. Hernalsteens, R. Tesse, and M. Vanwelde, *Zgoubidoo*, <https://ulb-metronu.github.io/zgoubidoo/>, 2022.
- [15] F. Asvesta, N. Karastathis, and P. Zisopoulos, *Pynaff: A python module that implements naff*, <https://github.com/nkarast/PyNAFF>, 2020.
- [16] L. Bojtár, “Frequency analysis and dynamic aperture studies in a low energy antiproton ring with realistic 3D magnetic fields,” *Physical Review Accelerators and Beams*, vol. 23, no. 10, p. 104002, 2020.  
doi:10.1103/PhysRevAccelBeams.23.104002
- [17] J. Laskar, “Frequency analysis for multi-dimensional systems. Global dynamics and diffusion,” *Physica D: Nonlinear Phenomena*, vol. 67, no. 1-3, pp. 257–281, 1993.  
doi:10.1016/0167-2789(93)90210-R
- [18] J. Laskar, “Frequency map analysis and particle accelerators,” in *Proc. PAC’03*, 2003, pp. 378–382.  
doi:10.1109/PAC.2003.1288929
- [19] F. Pedregosa *et al.*, “Scikit-learn: Machine learning in Python,” *Journal of Machine Learning Research*, vol. 12, pp. 2825–2830, 2011. doi:10.5555/1953048.2078195